Advances in Military Technology
Vol. 19, No. 1, 2024, pp. 5-23
ISSN 1802-2308, eISSN 2533-4123
DOI 10.3849/aimt.01865

# Optimization of the Route Determination Process for the Purposes of Military Terrain Passability

W. Dawid,* K. Pokonieczny and M. Wyszyński

*Institute of Geospatial Engineering and Geodesy, Faculty of Civil Engineering and Geodesy, Military University of Technology, Warsaw, Poland*

The manuscript was received on 8 November 2023 and was accepted after revision for publication as research paper on 13 March 2024.

**Abstract:**

*This paper presents a methodology for automated route determination in roadless terrains, optimizing it via digital elevation model (DEM) generalization, which forms the basis for route generation. Determining routes is a crucial aspect of planning and executing military or crisis management operations. The automated process employs high-resolution DEM and vehicle tractive parameters to determine routes in real-time, enabling generation of passability maps in unexplored areas. DEM generalization, based on local slope variations, expedites processing by reducing elevation points. Validated through research, this approach achieves a significant time reduction (approximately three times) while preserving route accuracy. User-adjustable parameters enhance the versatility of the algorithms for military and crisis management planning operations.*

**Keywords:**

*digital elevation model, generalization, terrain passability, routing, microrelief*

## 1 Introduction

The knowledge of topography is one of the key elements that should be taken into account while planning or conducting military operations. As far back as in the 6th century BC, the ancient Chinese philosopher Sun Tzu, in his book entitled "The Art of War", emphasized the importance of the terrain in military actions. Despite the fact that the military techniques have developed immeasurably throughout centuries, the importance of the terrain still remains unchanged, which was shown in previous studies [1, 2]. Nowadays, the influence of the terrain is determined in the intelligence preparation of the battlefield process (IPB), one of whose components is terrain analysis [3]. Its aim is to assess how the geographic environment impacts the military

* *Corresponding author: Institute of Geospatial Engineering and Geodesy, Faculty of Civil Engineering and Geodesy, Military University of Technology, Kaliskiego 2, PL 00-908 Warszawa, Poland. Phone: +48 535 22 58 44, E-mail: wojciech.dawid@wat.edu.pl. ORCID 0000-0001-7964-5706.*

operation. The paper [4] is a good example of what is included in terrain analysis in terms of geography. Moreover, the authors of the paper [5] demonstrated that the geographic information is indispensable to facilitate and accelerate the planning process in the selected tasks of military engineering.

Crucial task in terrain analysis is determining passability, defined by military standardization [6] as the ability of terrain to be navigated by various vehicles under diverse weather conditions. The analysis yields military passability maps, essential for planning military operations. In their simplest form, these maps categorize areas into GO, SLOW GO, and NO GO terrain classes [7]. Commanders use these maps to plan troop movements and military operations, selecting the most viable routes to avoid terrain obstacles and reach their objectives efficiently.

Passability maps offer detailed terrain information, with adjustability to suit different military operation levels. For the lowest tactical command levels, involving single or small groups of vehicles, microrelief analysis is crucial. The algorithm, detailed in [8], utilizes a high-resolution digital elevation model (DEM) and vehicle tractive parameters to identify impassable areas. These maps serve diverse purposes, including troop movement planning and route determination. The publication [9] illustrates the utilization of military passability maps for generating routes in various configurations.

Numerous authors have been investigating the development of military passability maps in recent years. One of the authors [10] described a system that can automatically develop military passability maps for the operational (mid-scale) level of command [11]. Research regarding the terrain passability was extended by investigating the influence of various factors on the passability conditions, including the vegetation [12-16] and the meteorological conditions [17]. Results of the forest passability analysis depend on the quality and topicality of the forest data, which was shown in paper [18]. Another important factor that influences the terrain passability is the type of soils. The impact of their parameters on possibilities of overcoming the terrain by specified vehicles is investigated in articles [19, 20]. Relief is also a pivotal factor which impacts the transport [21]. In paper [22], the author showed a concept for GIS based terrain mobility modelling and optimization of off-road route based on multiple factors, e.g. tree stands, roads and weather conditions. What is more, in the 1960s and 1970s, the NATO Reference Mobility Model (NRMM) project, regarding the modelling of cross-country movement, was developed. An extensive description of this model is presented in publication [23].

This study focuses on real-time microrelief analysis for determining routes in roadless areas tailored for specific vehicles. The broader topic of routing for cross-country vehicle movement has garnered attention from researchers, with methods presented in works like [24, 25], addressing uneven terrain, elevation models, and factors like friction, gravity, and maximum driving force. Multiple authors have utilized DEMs to develop or modify pathfinding algorithms for route determination in mobile robots and autonomous vehicles [26, 27]. An important consideration, highlighted in [28], explores how terrain surface data accuracy impacts the navigation of off-road military vehicles. This research contributes to improving route determination performance through DEM generalization – reducing elevation points subject to microrelief analysis. DEM generalization has been explored by various authors as well [29-31].

The focus of the presented studies was on route determination using various algorithms in different environments and generalizing DEM through different methods. In

contrast, this research combines the aspects which specifically address the process of determining routes based on a generalized DEM. Unlike the authors' previous work [9], which outlined optimal route determination using pre-generated military passability maps, this article introduces a novel method. The primary objective is to develop a technique that relies solely on high-detail generalized DEM to determine real-time routes between two points, considering relief conditions without the necessity for pre-prepared passability maps.

Prior research by the authors [32] highlighted the slowness of microrelief analysis, despite its detailed outcomes in determining impassable areas. Consequently, the subsequent goal was to enhance the performance of microrelief analysis and reduce route generation time. This was accomplished through DEM generalization, which decreases elevation points in areas with minimal relief diversification, measured by local slope variations. While previous articles discussed various DEM generalization methods for topography representation, this work uniquely focuses on optimization of subsequent processes rather than solely topographic representation.

Taking into consideration the above, the following research questions can be formulated: can the DEM generalization improve the performance of the route determination process while maintaining its accuracy and if so, by how much?

## 2 Materials and Methods

The iterative route determination process involves microrelief analysis based on a highly detailed DEM to identify impassable microrelief objects (pits, drainage ditches, bluffs, etc.) and to ensure that the route avoids these obstacles for a given vehicle model. The high detail, at a 1 m resolution, results in a large number of elevation points, potentially causing lengthy analyses based on the route length. To address this, a DEM generalization methodology was developed. This approach reduces elevation points, shortening the analysis duration while preserving model detail. This section provides a detailed description of both the generalization and iterative route determination methodologies.

### *2.1 Data Used in the Experimentation*

The research utilized LIDAR (Light Detection and Ranging) elevation data obtained from the Polish Head Office of Geodesy and Cartography via the National Geodesy and Cartography Resource. These data, available in ASCII grid file format, provide three-dimensional coordinates of elevation points with a 1 m spacing. Accessible for free on the governmental website (www.geoportal.gov.pl) covering Poland's entire territory, the data boast a stated vertical accuracy of 0.15 m. Due to the data being from 2011, terrain verification was conducted to ensure quality, as detailed in Section 3.3.

The tests were conducted for the Honker 2000 vehicle, which is widely used in the Polish Armed Forces. It is a Polish off-road passenger vehicle which has the following tractive parameters: wheelbase – 2.90 m; track width – 1.65 m; ground clearance – 0.22 m. These parameters will be used in the methodology to perform the microrelief analysis and determine the impassable areas for this vehicle.

### 2.2 Study Area

The study focused on an area in Lebork County, northern Poland, encompassing nearly 0.16 km$^2$ with an altitude range from 7.3 m to 9.7 m above mean sea level (MSL). The terrain features a network of drainage ditches, posing potential impassability for the analyzed vehicle and challenging the route determination process. Additionally, the area includes culverts, which may facilitate vehicle passage. The presence of these microrelief objects makes this selected area suitable for testing the developed methodologies. The location and characteristic objects of the area are presented in Fig. 1.

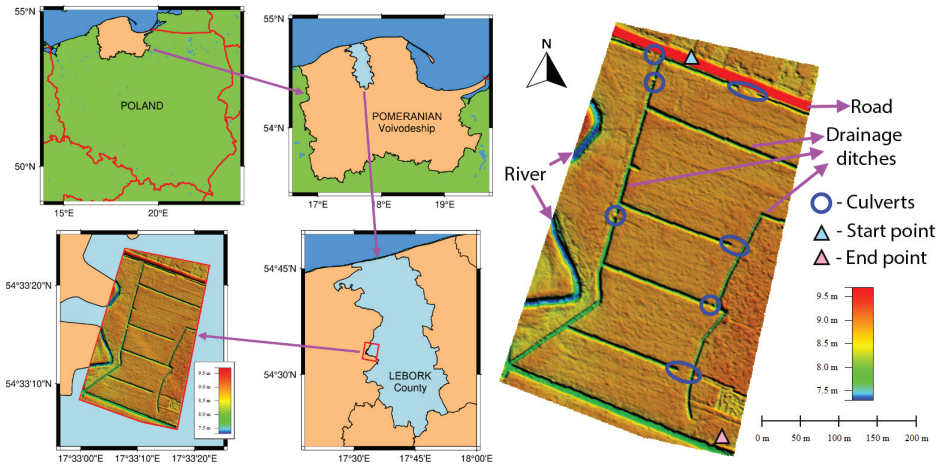


*Fig. 1 Location of the study area and its characteristic objects*

### 2.3 Digital Elevation Model Generalization

The route determination process involves a slow microrelief analysis at each point of the DEM along its hypothetical course, as demonstrated in [32]. To optimize and expedite the analysis, DEM generalization was employed. This process assumes that terrain in uniform relief areas can be represented with fewer elevation points. Conversely, in areas with greater relief variations, the number of elevation points should remain unchanged. These assumptions enable a faster route determination process and microrelief analysis, reducing the number of points analyzed. The process has been automated in a form of a plugin to QGIS software and it was written in Python programming language. The workflow of the generalization process is presented in Fig. 2.

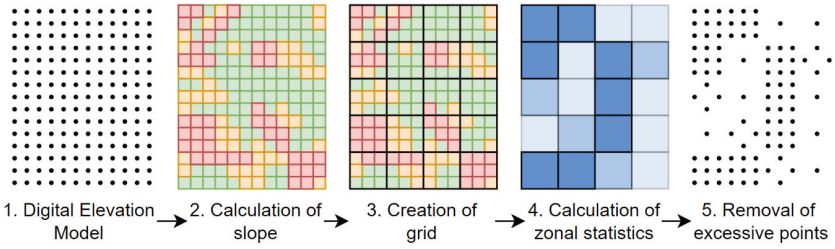


*Fig. 2 Digital elevation model generalization process*

One may see that the whole DEM generalization process consists of five main steps. The detailed description of each of them is presented in the points below.

- DEM import: at the beginning, the process imports the DEM in ASCII grid file format in order to perform further operations on it. As it was already mentioned, the model consists of elevation points distributed evenly as a grid with 1 m spacing.
- Calculation of the slope: the second step calculates the slope on the basis of imported DEM. The slope values allow for the identification of local variations of terrain heights.
- Creation of the grid: on the basis of the extent of analyzed DEM, the additional grid is generated. It consists of single cells and its aim is to create areas (bigger than the resolution of DEM) where the zonal statistics will be calculated. The cells can be generated in various shapes and sizes. In this research there were nine configurations of examined cells in total (sizes: 5 m, 10 m, 15 m; shapes: rectangle, diamond, hexagon). On the basis of this diversification, the dependencies between various configurations of the grid and the final generalized DEM will be examined.
- Calculation of zonal statistics: the following step consists of the calculation of zonal statistics in each cell. This research assumes that the generalization of DEM is conducted on the basis of relief diversification in each cell. The indicator that measures the variability of values (in this case the slopes) is standard deviation. It indicates fluctuations of the terrain heights in a given cell. It means that the bigger the relief diversification, the higher the standard deviation is. On the basis of this indicator, the following step will be performed.
- Removal of excessive points: the number of removed points within each cell depends on the calculated standard deviation. Initially, all cells are classified into several classes based on this value. The number of classes can be set in the plugin and in this research, three variations were used: 6, 8, and 10 classes. The additional parameter, which is utilized in computation of ranges of standard deviations within each class, is the standard deviation threshold (denoted later as SDT). In cells with the statistic value above this threshold no elevation points are removed. This parameter is also adjustable; in this research three threshold values were used for testing: 3°, 4.5°, and 6°. The plugin, having defined the number of classes and the threshold value, removes the elevation points in inverse proportion to the standard deviation in each class. An example is presented in Fig. 3.

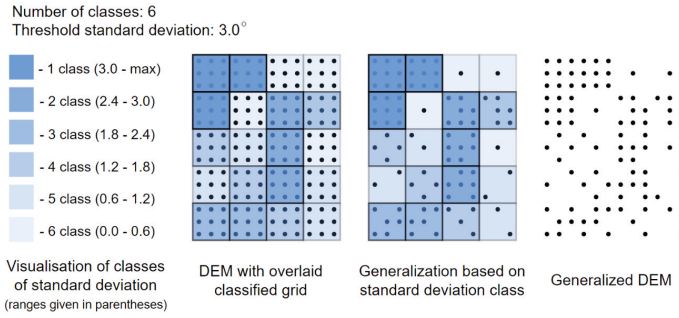


*Fig. 3 The removal of excessive elevation points*

To sum up, the generalization of the DEM can be adjusted in the plugin by 4 parameters: shape of cell, size of cell, number of classes, and SDT. For the tests, generalized models were generated for the following settings: shape and size; number of classes – 6, 8, and 10; SDT – 3°, 4.5°, and 6°. All results are analyzed in further part of the article.

### *2.4 Iterative Route Determination*

As part of further research, a program in Python programming language was developed that enables to determine route between two points iteratively, taking into account microrelief objects in real-time. The methodology of this process will be explained based on Fig. 4.

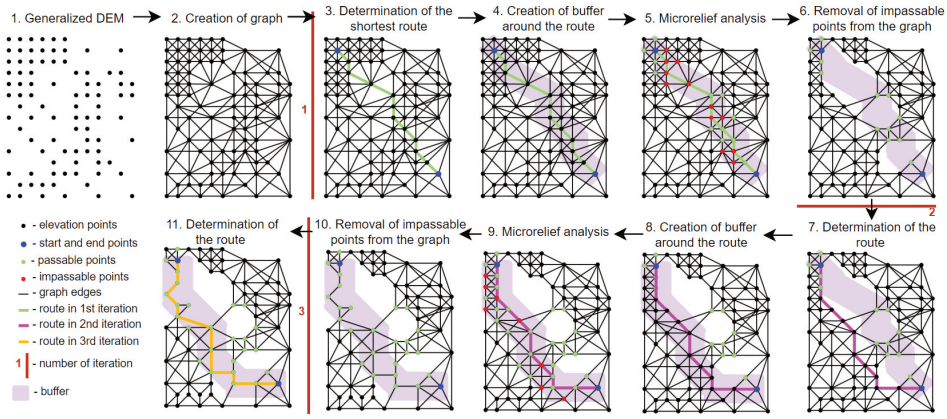


*Fig. 4 Workflow of the route determination process*

The illustration above shows the execution of each step of the route determination process in three iterations. Their number strictly depends on the presence of microrelief objects, which must be avoided mostly by the route. The whole algorithm will be described in following points:

- Import of the generalized DEM: in the initial phase of the process, the program imports the generalized DEM. Apart from it, the algorithm also requires the coordinates of the start and end points of the route and the type of vehicle for which the route will be determined. These data are necessary for the computation of microrelief analysis and they are provided by the user of the program.
- Creation of graph: on the basis of the DEM, a graph is created, which consists of nodes and edges. Nodes are elevation points and edges are the lines that connect them. Because of the fact that the elevation points in the generalized DEM are not distributed evenly and the distances between them vary, the graph was generated with the use of the k-nearest neighbors method. It connects a specified number of nodes that are located in the neighborhood to a given node. This number was set to eight because in the areas with the highest density of nodes they create a regular grid with 1 m spacing in orthogonal manner and each node is surrounded by eight neighboring nodes that must be connected.
- Determination of the shortest route – first iteration: subsequently, the shortest route between the start and end point is determined with the use of the well-known and commonly used Dijkstra pathfinding algorithm. This step begins the

first iteration of the whole route determination process. The Dijkstra algorithm realizes the so-called greedy approach which means that in each iteration one of the unvisited nodes, which can be reached at the lowest cost, is chosen. The algorithm does not analyze the influence of the current action on the further steps of determining the route; however, it selects the locally optimal solution [33]. Other pathfinding algorithms, e.g. A-star, were not taken into account because the publication [9] showed that Dijkstra gives better results.

- Creation of a buffer around the determined route: the next step uses the determined route to create a buffer around it. The buffer is used to select elevation points for the microrelief analysis. Its size can be adjusted in the program and for tests it was set to 10 m.
- Microrelief analysis: this step involves analyzing microrelief at each point within the buffer boundaries. It checks the passability of the terrain for a specific vehicle, considering tractive parameters and the elevation model. The analysis assesses whether the vehicle can traverse the terrain without getting stuck on microrelief objects like drainage ditches, embankments, or pits. Detailed information on this process is available in [32]. In this research, the microrelief analysis utilizes the current azimuth of the determined route, positioning the vehicle appropriately and aligning the chassis plane correctly. The buffer restricts the number of analyzed elevation points, improving analysis performance. Each analyzed elevation point is subsequently classified as passable or impassable.
- Removal of impassable points (nodes) from the graph: having analyzed the microrelief, all impassable nodes and all edges that interconnect them are removed from the graph. Then, the algorithm checks if there is a possibility to determine a route based on the remaining nodes inside the buffer. As one may see in Fig. 4 (step no. 6), there is no possible way to generate a route within the buffer, so this situation triggers the second iteration.
- Determination of the shortest route – second iteration: this step starts the second iteration of the whole process and utilizes the Dijkstra algorithm to determine the shortest route between the start and end point based on the reduced graph.
- Creation of a buffer around the determined route: subsequently, a buffer is created around the newly created route. It can overlap with the previously generated one (step no. 4), and consequently, the same elevation points, which have been analyzed yet, may be taken into the microrelief analysis. However, the algorithm does not take into account previously analyzed points, so that no redundant operations are performed on the same point. This improves the performance of the algorithm.
- Microrelief analysis: the microrelief analysis is performed at each unanalyzed point within the buffer.
- Removal of impassable points (nodes) from the graph: this step enables to remove impassable nodes from the graph and reduce it even more. Then, the algorithm checks whether there is a connection between the start and end points inside the buffer. One may see that in this case there is a possible connection within the buffer.
- Determination of the shortest route – third iteration: the start of the subsequent iteration is again the determination of the shortest route between two points. If there is a possibility to connect those points within the buffer (like in this case),

the algorithm determines such route and ends the whole process. Otherwise, the process continues until a connection within the buffer is maintained. Having determined the route, the program exports it in Shapefile format to a destination folder defined by the user.

### *2.5 Terrain Verification*

Due to the fact that the data used in the analysis are from the year 2011, field measurements were taken to verify them. They were done with the use of GNSS (Global Navigation Satellite Systems) technology using Leica VIVA GS15 receiver. The RTK (Real Time Kinematic) method was applied, which allowed us to measure with an accuracy of not exceeding 0.03 m both vertically and horizontally. To calculate the accuracy of the DEM, 300 control points were measured. Then they were compared to the heights from this model. The height accuracy was measured by the RMSE (Root Mean Square Error). Additionally, photographic documentation was collected in order to assess visually whether the determined route is passable and the profiles of microrelief objects were measured.

## 3 Results

The outcome of the conducted research can be divided into two parts. The first part concerns the DEM generalization and the second contains the results of the route determination process. This section only presents the obtained results. Their analysis is thoroughly described in section 4.

### *3.1 Results of the DEM Generalization*

The generalization of the DEM was performed for various settings (shape and size of cells, number of classes and SDT). Due to the large number of results, only some of them will be shown, i.e. those that present the dependencies between various settings (Fig. 5). As an estimator that describes the level of generalization, the degree of generalization (*DEG_GEN*) coefficient was calculated with the use of Eq. (1).

$$DEM\_GEN = (1 - N_{gen\_DEM} / N_{DEM}) \cdot 100\ \% \tag{1}$$

The degree of generalization is a percentage value, which is calculated based on $N_{gen\_DEM}$ – number of elevation points in the generalized DEM and $N_{DEM}$ – number of elevation points in the original non-generalized DEM. It enables to determine how various parameters influence the number of the removed elevation points. The higher the *DEG_GEN*, the more elevation points were removed from the original DEM.

The degrees of generalization of all generalized DEMs generated in each configuration of parameters are presented in Tab. 1.

### *3.2 Results of Route Determination Process*

Between start and end points of the route, there are a lot of terrain obstacles, such as drainage ditches, which are likely to be classified as impassable for the analyzed vehicle. Hence, the algorithm had to perform multiple iterations in order to find a direct connection between the start and end points while avoiding those impassable areas. Fig. 6 displays selected predetermined routes and the reference route determined using the non-generalized DEM.

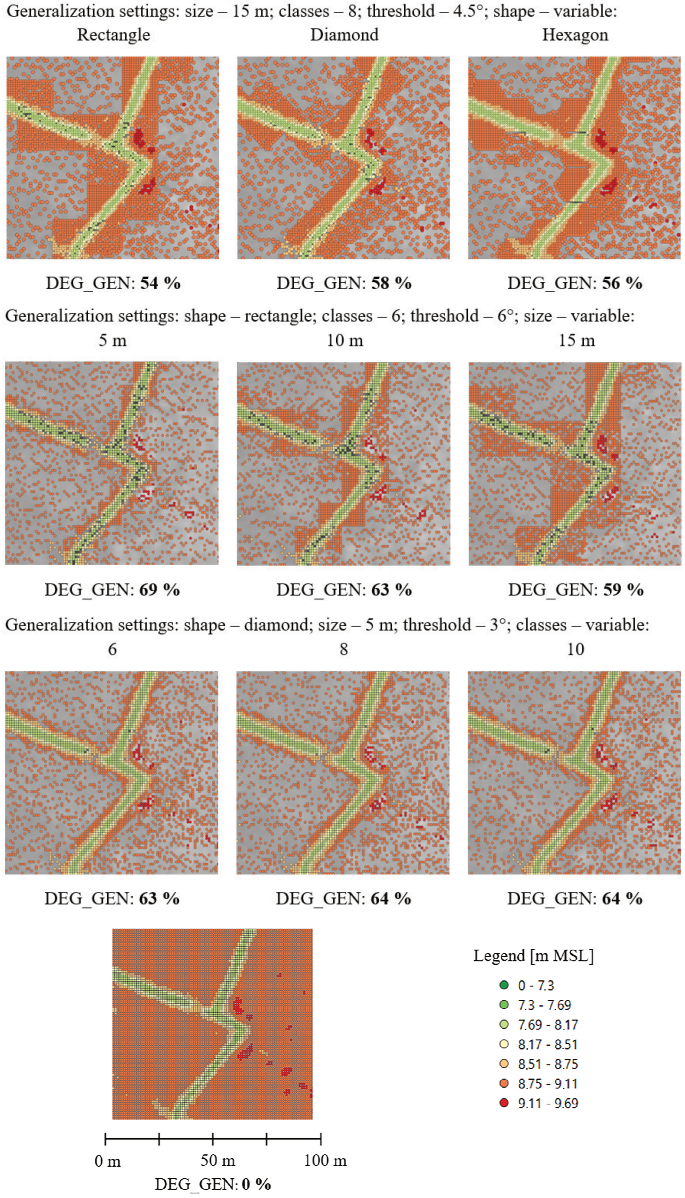


*Fig. 5 Visualization of selected results of DEM generalization*

The reference route was determined on the basis of the non-generalized DEM and thus it will be used for comparing routes which were generated based on the generalized DEMs. One may see in Fig. 6 that the determined routes are generally very similar both to each other and to the reference route. However, in some cases, the route crosses the microrelief objects. They will be treated as inappropriate solutions because the reference route visibly avoids all those obstacles, which means that they should not be crossed. Moreover, to check the deviations between the reference route and each determined route, the area between those two objects was calculated. The

more similar the course of the determined route to the course of the reference route is, the smaller the area between them is. Tab. 2 presents area values for routes determined on the basis of the generalized DEMs of the given parameters and indicates the routes (marked in red) that were determined incorrectly (i.e. those that cross microrelief objects).

*Tab. 1 Degrees of generalization of all generalized DEMs [%]*

| Number of points in the non-generalized DEM: **152 593** | | | Number of classes and standard deviation threshold | | | | | | | | |
|---|---|---|---|---|---|---|---|---|---|---|---|
| | | | 6 classes | | | 8 classes | | | 10 classes | | |
| | | | 3° | 4.5° | 6° | 3° | 4.5° | 6° | 3° | 4.5° | 6° |
| Shape and size of cells | Rectangle | 5 m | 60 | 65 | 69 | 60 | 67 | 72 | 60 | 67 | 73 |
| | | 10 m | 52 | 58 | 63 | 51 | 59 | 65 | 52 | 59 | 65 |
| | | 15 m | 46 | 53 | 59 | 45 | 54 | 61 | 46 | 53 | 61 |
| | Diamond | 5 m | 63 | 69 | 72 | 64 | 71 | 75 | 64 | 71 | 76 |
| | | 10 m | 66 | 70 | 74 | 66 | 71 | 76 | 66 | 72 | 76 |
| | | 15 m | 51 | 57 | 63 | 51 | 58 | 64 | 51 | 58 | 65 |
| | Hexagon | 5 m | 64 | 69 | 73 | 64 | 70 | 75 | 64 | 71 | 76 |
| | | 10 m | 53 | 59 | 64 | 53 | 60 | 66 | 53 | 60 | 66 |
| | | 15 m | 49 | 55 | 61 | 48 | 56 | 62 | 49 | 55 | 63 |

*Tab. 2 Areas between reference route and each determined route as well as marked incorrect routes*

| Area [1 000 m$^2$] Incorrect routes marked in red | | | Number of classes and standard deviation threshold | | | | | | | | |
|---|---|---|---|---|---|---|---|---|---|---|---|
| | | | 6 classes | | | 8 classes | | | 10 classes | | |
| | | | 3° | 4.5° | 6° | 3° | 4.5° | 6° | 3° | 4.5° | 6° |
| Shape and size of cells | Rectangle | 5 m | 0.07 | 0.20 | 3.21 | 0.04 | 0.98 | 0.77 | 0.20 | 0.14 | 2.18 |
| | | 10 m | 2.07 | 0.80 | 0.54 | 1.77 | 1.84 | 2.16 | 1.51 | 1.37 | 0.23 |
| | | 15 m | 2.04 | 0.89 | 1.54 | 1.83 | 2.51 | 1.89 | 2.72 | 1.01 | 0.80 |
| | Diamond | 5 m | 1.67 | 1.28 | 0.79 | 0.60 | 12.23 | 1.98 | 1.51 | 0.85 | 1.38 |
| | | 10 m | 1.75 | 0.55 | 1.33 | 0.51 | 2.16 | 20.56 | 0.63 | 2.11 | 0.73 |
| | | 15 m | 1.76 | 0.74 | 1.51 | 0.70 | 3.36 | 2.25 | 1.61 | 1.02 | 0.63 |
| | Hexagon | 5 m | 0.95 | 1.79 | 0.11 | 0.47 | 0.49 | 1.82 | 0.70 | 0.97 | 1.82 |
| | | 10 m | 0.54 | 1.58 | 0.03 | 1.02 | 0.33 | 1.09 | 0.66 | 1.10 | 0.65 |
| | | 15 m | 2.07 | 0.92 | 0.56 | 1.24 | 1.04 | 1.09 | 2.78 | 0.04 | 1.05 |

One may see that there are 8 incorrectly determined routes out of 81 in total, which gives over 90 % efficiency in determining the route.

### *3.3 Results of Terrain Verification*

As it was already mentioned, 300 randomly distributed control points were measured in the terrain. As a result, an accuracy of 0.19 m was obtained, which slightly exceeds the accuracy of the information provided by the data distributor. The probable reason of this error is the outdatedness of the older elevation data. Throughout the years a lot of factors might have influenced the shaping of this area.

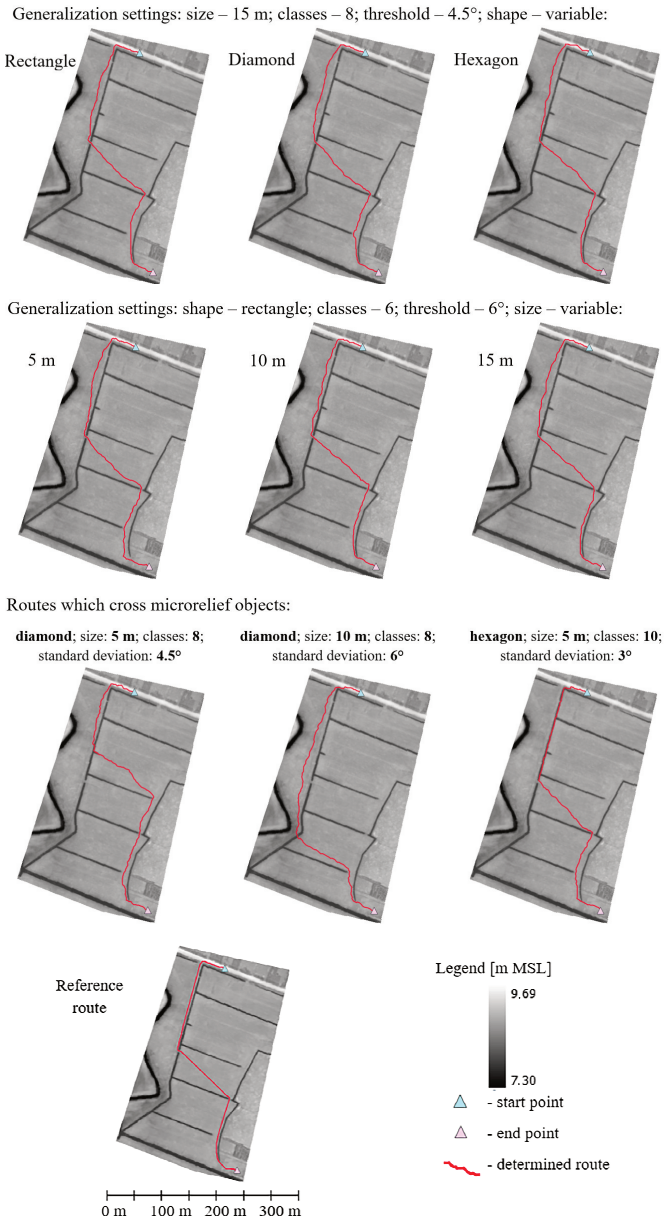


*Fig. 6 Visualization of the selected determined routes*

However, the analysis of the archival ortophotomap of this area from 2011 year (the year the elevation data are from) proved that this terrain had not changed. The same microrelief objects were present as at the time of this research. What is more, this area is used for agricultural purposes, so the machinery working on it might have had a significant influence on this accuracy error. Nevertheless, the obtained accuracy of the DEM does not exceed the accuracy of the data provider so much that the model

should be excluded from performing the analysis. The terrain verification also involved taking photographs of the terrain (Fig. 7).

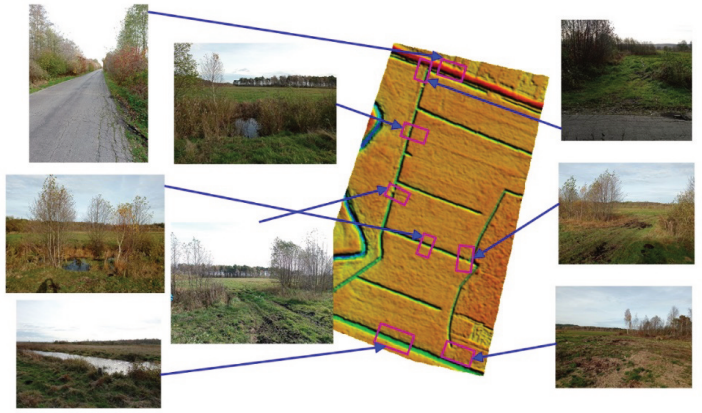

*Fig. 7 Photographs of marked parts of the analyzed terrain*

## 4 Discussion

Generally speaking, the obtained results demonstrated that the developed methodology made it possible to determine routes iteratively on the basis of the generalized DEMs. It was also noticeable that the use of various parameters enabled to obtain DEMs of different degrees of generalization. Consequently, these models led to the determination of routes with mostly similar, but not the same, courses. These observations will be described in detail in this section.

### *4.1 Generalized DEMs*

The obtained results showed that the degree of generalization ranges from 45 % to 76 % depending on the used parameters, with a mean of 62 %. This value means that the overall number of elevation points was reduced from 152 593 (in the non-generalized DEM) to 94 608 on average. Obviously, the degree of generalization depends mainly on the terrain for which the generalization is performed. The methodology assumes that the number of removed elevation points is in inverse proportion to the standard deviation of slopes on a given area, so the more diversified the terrain, the bigger the standard deviation, and, in consequence, fewer elevation points are removed. The dependencies between the degrees of generalization and various parameters applied to the generalization are presented in Figs 8-10.

Based on the charts presented above, one may conclude that with the growth of size of the cells, the degree of generalization decreases in almost each case (Fig. 8). Diamond shape is an exception from this dependence because it has the biggest degree of generalization in 10 m cell. The reason why the degree of generalization is dropping while increasing the cell size is the fact that the microrelief objects are usually several meters in size and even if they occupy a small part of a bigger cell (e.g. a 3 m wide drainage ditch located in a 15 m cell) they increase the standard deviation of slope in this field. Consequently, this cell is assigned to a class with higher standard deviation, which results in the removal of fewer elevation points. Thus, having the terrain divid-

ed into smaller cells, fewer areas are assigned to higher classes of standard deviation, and subsequently, the degree of generalization increases.

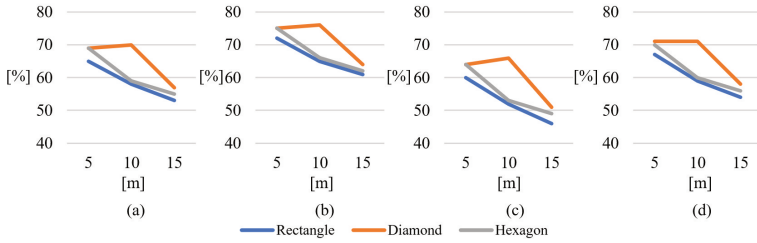


*Fig. 8 Dependence between DEG_GEN and the size of cells for various shapes in DEMs with the following parameters: (a) 6 classes and* 4.5° *SDT; (b)* 8 *classes and* 6° *SDT; (c)* 10 *classes and* 3° *SDT; (d)* 8 *classes and* 4.5° *SDT*

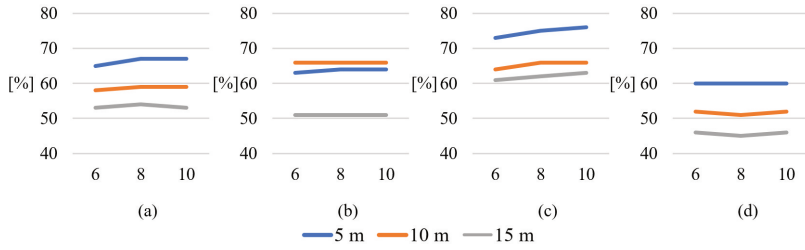


*Fig. 9 Dependence between the DEG_GEN and the number of classes for various sizes of cells in DEMs with the following parameters: (a) rectangle shape and* 4.5° *SDT; (b) diamond shape and* 3° *SDT; (c) hexagon shape and* 6° *SDT; (d) rectangle shape and* 3° *SDT*

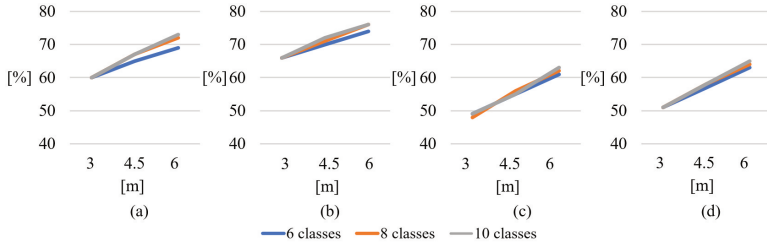


*Fig. 10 Dependence between the DEG_GEN and SDT for various number of classes in DEMs with the following parameters: (a) rectangle and* 5 m *size; (b) diamond and* 10 m *size; (c) hexagon and* 15 m *size; (d) diamond and* 15 m *size*

Moreover, the increase of the number of classes has no or only slight influence on the degree of passability in each analyzed size of the cell (Fig. 9). On the other hand, the rise of the standard deviation threshold causes the growth of the degree in each number of classes (Fig. 10). This figure also shows that the lines presenting various numbers of classes are mostly overlapping. It means that changing the number of classes has no or only little influence on the obtained results. The difference between the degrees of generalization in this case is negligible and does not exceed 4 % in any case. The figures above (Figs 8-10) show only some examples from the whole collec-

tion of results but the visible rules, which can be inferred from them, represent their holistic character accurately.

### *4.2 Determined Routes*

The iterative route determination process resulted in obtaining two products: the shortest route between the start and end points, which leads through areas defined as passable for the specified type of vehicle, as well as a point layer with indicated impassable elevation points in each iteration. An exemplary result is presented in Fig. 11.

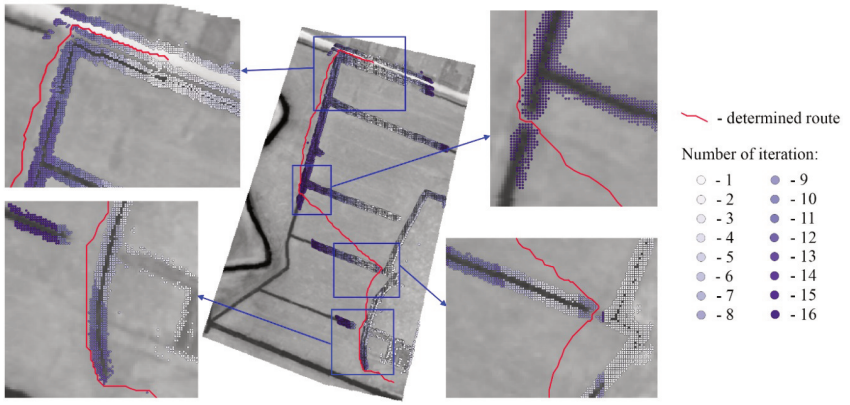


*Fig. 11 Determined route and impassable elevation points in each iteration*

Impassable points, mainly along drainage ditches, were effectively navigated by the algorithm which strategically passed through culverts. The algorithm exhibited extensive computation, evident in the mean of 16 iterations across all cases. Fig. 11 illustrates the iteration order, intensifying color to denote changes. Initially, the route followed a straight line from the start to the end. Upon encountering microrelief obstacles, deviations occurred on both sides before the algorithm found a viable passage, ultimately determining the route.

Regarding route variations, Tab. 2 illustrates the differences between routes determined from the reference route (non-generalized DEM) and those based on generalized DEMs. The discrepancies do not surpass 3 360 $m^2$ for correctly determined routes. Notably, no discernible dependencies exist between these variations and the generalization parameters used. Diverse routes result from variations in elevation point disposition in generalized DEMs (Fig. 5). Despite this diversity, all routes navigate through the same culverts. Remarkably, inaccuracies in route determination primarily occurred with generalized DEMs in diamond and, to a lesser extent, hexagon shapes. Rectangular cell-shaped generalized DEMs demonstrated no inaccuracies, establishing them as the most reliable shape.

### *4.3 Performance of the Program*

In order to check how the DEM generalization affected the time of the route determination, performance tests were conducted. They were executed on two machines with various parameters (Tab. 3).

*Tab. 3 Machines used for performance tests*

| Name | Processor | Base frequency | RAM | Number of cores |
|---|---|---|---|---|
| Machine A | AMD Ryzen 7 4800H | 2.90 GHz | 16 GB | 8 |
| Machine B | 2 x Intel® Xeon® Gold 6230 | 2.10 GHz | 192 GB | 40 |

Tests involved route determination using a non-generalized DEM and three generalized DEMs at 45 %, 62 %, and 76 % degrees of generalization representing minimum, mean, and maximum values. Performance tests were conducted both with and without multiprocessing. Multiprocessing divides computations into simultaneous subprocesses, utilizing all CPUs and achieving 100 % CPU utilization throughout. In contrast, non-multiprocessing involves single-process execution, leading to low CPU utilization as only one CPU is utilized. Results of the performance tests are presented in Tab. 4.

*Tab. 4 Machines used for performance tests (multiprocessing denoted as MP)*

| Duration of process [hh:mm:ss] | | Machine A | | Machine B | |
|---|---|---|---|---|---|
| | | no MP | with MP | no MP | with MP |
| non-generalized DEM | | 02:15:30 | 00:53:33 | 03:18:52 | 00:24:33 |
| generalized DEMs [*DEG_GEN*] | 45 % | 01:05:02 | 00:27:09 | 01:36:09 | 00:14:58 |
| | 62 % | 00:49:32 | 00:19:18 | 01:06:14 | 00:11:08 |
| | 76 % | 00:36:27 | 00:16:45 | 00:46:08 | 00:08:26 |

The processing times demonstrate a substantial impact from multiprocessing. Machine B experienced an impressive 8× reduction in processing time for non-generalized DEM and a 5.5× reduction for the most generalized DEM. Machine A, with fewer CPUs, showed less significant time savings. Additionally, the processor's base speed significantly influenced performance without multiprocessing. On Machine A, with a higher base speed, processing times were faster, reduced by approximately 32 % for non-generalized DEM and 22 % for the most generalized one.

Moreover, the number of CPUs has the biggest impact on the processing time. Despite having lower base speed, the machine is able to divide the whole process into more subprocesses and execute them simultaneously, thus significantly reducing the processing time. Faster processors with more CPUs would allow even larger reduction.

## 5 Conclusions

The conducted research has demonstrated that the developed methodologies are able to, firstly, determine the routes taking into account the microrelief obstacles in real-time and, secondly, significantly reduce the duration of this process by the DEM generalization. As far as the latter is concerned, Fig. 5 and Tab. 1 show that the results of the generalization process differ from each other depending on the used parameters. The factor that has the least influence is the number of classes of standard deviations, which means that it may be omitted while determining the generalization parameters. Other variables (shape and size of the cell, standard deviation threshold) cause the intensification or reduction of the degree of generalization. It depends on the user of the program which parameters should be set in this process. The possibility of changing the generalization parameters makes this algorithm universal and therefore it may

be used to optimize various purposes and processes, which utilize the high resolution DEM. Moreover, the comparison between the reference (non-generalized) DEM and the generalized ones showed that the generalization process did not affect their accuracy in the analyzed area. The differences were mostly (99.9 %) within the 0.15 m range, which is the accuracy provided by the data distributor.

The routing problem between two points on the undeveloped area has been solved by the iterative route determination algorithm. A big advantage of this algorithm is that it needs only a high resolution DEM, which can be obtained from the governmental website free of charge, and the tractive parameters of the vehicle, for which the route is generated. The algorithm checks the passability conditions in real-time and avoids impassable areas iteratively looking for a connection between the start and end points. In a variable environment, e.g. battlefield, the usage of this program can be crucial because, provided that the updated DEM can be acquired, it will be able to determine new routes taking into account the current terrain conditions. Contrary to previous routing solutions presented in [10], this method operates on the terrain which has not been investigated in terms of passability yet. As a result, it is independent of the time-consuming passability analysis which would have to be performed primarily.

Regarding the route determination process duration, the performance test revealed a significant reduction through DEM generalization. Increasing the generalization degree of the DEM resulted in decreased processing time. Multiprocessing played a crucial role, with simultaneous execution of several subprocesses yielding a performance increase of over 8 times. Notably, the analyzed area covered approximately 0.16 $km^2$, and the straight-line distance between start and end points was 490 m, expanding to about 675 m after route determination. Operational use in larger areas may incur longer processing times. Additionally, the number of iterations, influenced by terrain features like drainage ditches, averaged 16, impacting the processing speed. The findings suggest the program's applicability in diverse fields, including military operations and crisis management planning. Performance enhancements are evident with better computing machines featuring more and faster CPUs.

In conclusion, the proposed DEM generalization methodology may be applied to analyses requiring an elevation model, to reduce its duration. Despite the fact that it was not tested in real terrain conditions and for other terrain types that can be found in the world, the generalization may be applied to other elevation sources with similar quality and structure of data as the tested dataset. It would be worth checking in further research whether this method might be applied to the lower resolution data, such as DTED (Digital Terrain Elevation Data), SRTM (Shuttle Radar Topographic Mission) or TREx (TanDEM-X High Resolution Elevation Data Exchange). The generalization allowed the authors to perform the route determination process faster by about 3 times, which may occur to be critical for the success of any military or crisis management operation. However, the research does not encompass the speed of vehicle movement, which can be a crucial factor in effective time management in operational planning. Further research should focus on the implementation of soils and weather conditions to the passability analysis, which would allow to determine the passability (and consequently the routes) for the near future based on weather forecasts and perform this analysis on various areas of different characteristics, e.g. mountainous, urban or forested areas. Such issues would cover other aspects that are important from the military or crisis management point of view.

## Acknowledgement

This work was supported by Military University of Technology in Warsaw, Faculty of Civil Engineering and Geodesy, Institute of Geospatial Engineering and Geodesy: [University Research Grant for 2024].

## References

[1] DOYLE, P. and M.R. BENNETT. *Fields of Battle: Terrain in Military History*. Dordrecht: Springer, 2002. ISBN 978-94-017-1550-8.

[2] ROSKIN, J. The Role of Terrain and Terrain Analysis on Military Operations in the Late Twentieth to Early Twenty-First Century: A Case Study of Selected IDF Battles. In: *Military Geoscience: Bridging History to Current Operations*. Cham: Springer, 2020, pp. 145-160. ISBN 978-3-030-32172-7.

[3] *ATP 2-01.3. Intelligence Preparation of the Battlefield* [online]. 2014 [viewed 2022-02-10]. Available from: https://www.marines.mil/portals/1/MCRP%202-10B.1.pdf?ver=2018-10-04-131000-610

[4] HEŠTERA, H. and M. PAHERNIK. Physical-Geographic Factors of Terrain Trafficability of Military Vehicles According to Western World Methodologies. *Croatian Geographical Bulletin*, 2018, **80**(2), pp. 5-31. DOI 10.21861/HGG.2018.80.02.01.

[5] SEDLÁČEK, M. and F. DOHNAL. Possibilities of Using Geographic Products in Tasks of Military Engineering. *Challenges to National Defence in Contemporary Geopolitical Situation*, 2020, **2020**(1), pp. 145-155. DOI 10.47459/cndcgs.2020.18.

[6] NO-06-A015:2012, *Polish Ministry of National Defence*, *Terrain – Rules of Classification – Terrain Analysis on Operational Level*.

[7] *Terrain Analysis*, *Army Field Manual No. 5-33* [online]. 1990 [viewed 2022-02-15] Available from: https://ia600304.us.archive.org/5/items/milmanual-fm-5-33-terrain-analysis/fm_5-33_terrain_analysis.pdf

[8] DAWID, W. and K. POKONIECZNY. Automation of the Terrain Classification Process due to Passability Taking the Microrelief Shapes into Consideration. In: *2021 International Conference on Military Technologies (ICMT)*. Brno: IEEE, 2021, pp. 1-8. DOI 10.1109/ICMT52455.2021.9502821.

[9] DAWID, W. and K. POKONIECZNY. Methodology of Using Terrain Passability Maps for Planning the Movement of Troops and Navigation of Unmanned Ground Vehicles. *Sensors*, 2021, **21**(14), 4682. DOI 10. 3390/s21144682.

[10] POKONIECZNY, K. Automatic Military Passability Map Generation System. In: *2017 International Conference on Military Technologies (ICMT)*. Brno: IEEE, 2017, pp. 285-292. DOI 10.1109/ MILTECHS.2017.7988771.

[11] HOHMANN, A., G. GRANDJEAN, V. MARDHEL, G. SCHAEFER and N. DESRAMAUT. A GIS-based Vehicle Mobility Estimator for Operational Contexts. *Transactions in GIS*, 2013, **17**(1), pp. 78-95. DOI 10.1111/j.1467-9671.2012.01351.x.

[12] HUBACEK, M., L. CEPLOVA, M. BRENOVA, T. MIKITA and P. ZERZAN. Analysis of Vehicle Movement Possibilities in Terrain Covered by Vegetation.

In: *2015 International Conference on Military Technologies (ICMT)*. Brno: IEEE, 2015, pp. 1-5. DOI 10.1109/MILTECHS.2015.7153730.

[13] CAPEK, J., P. ZERZAN and K. SIMKOVA. Influence of Tree Spacing on Vehicle Manoeuvers in Forests. In: *2019 International Conference on Military Technologies (ICMT)*. Brno: IEEE, 2019, pp. 1-7. DOI 10.1109/MILTECHS. 2019.8870092.

[14] RYBANSKY, M. Determination the Ability of Military Vehicles to Override Vegetation. *Journal of Terramechanics*, 2020, **91**, pp. 129-138. DOI 10.1016/ j.jterra. 2020.06.004.

[15] RYBANSKY, M. Determination of Forest Structure from Remote Sensing Data for Modeling the Navigation of Rescue Vehicles. *Applied Sciences*, 2022, **12**(8), 3939. DOI 10.3390/app12083939.

[16] RYBANSKY, M., M. BRENOVA, J. CERMAK, J. VAN GENDEREN and Å. SIVERTUN. Vegetation Structure Determination Using LIDAR Data and the Forest Growth Parameters. *IOP Conference Series: Earth and Environmental Science*, 2016, **37**, 12031. DOI 10.1088/1755-1315/37/1/012031.

[17] HUBÁČEK, M., V. KOVARIK, V. TALHOFER, M. RYBANSKY, A. HOFMANN, M. BRENOVA and L. CEPLOVA. Modelling of Geographic and Meteorological Effects on Vehicle Movement in the Open Terrain. In: *Proceedings of 23rd Central European Conference.* Brno: Masarykova univerzita, 2016, pp. 149-159. ISBN 978-80-210-8313-4.

[18] RADA, J., M. RYBANSKY and F. DOHNAL. Influence of Quality of Remote Sensing Data on Vegetation Passability by Terrain Vehicles. *ISPRS International Journal of Geo-Information*, 2020, **9**(11). DOI 10. 3390/ijgi9110684.

[19] RYBANSKY, M. Soil Trafficability Analysis. In: *International Conference on Military Technologies (ICMT) 2015*. Brno: IEEE, 2015, pp. 1-5. DOI 10.1109/MILTECHS. 2015.7153728.

[20] HUBÁČEK, M., M. RYBANSKY, K. CIBULOVA, M. BRENOVA and L. CEPLOVA. Mapping the Passability of Soils for Vehicle Movement. *KVÜÕA Toim*, 2016, **21**, pp. 5-18.

[21] RYBANSKY, M. and M. VALA. Relief Impact on Transport. In: *2009 International Conference on Military Technologies (ICMT)*. Brno, 2009, pp. 1-9. ISBN 978-80-7231-649-6.

[22] SUVINEN, A., M. SAARILAHTI and T. TOKOLA. Terrain Mobility Model and Determination of Optimal Off-Road Route. In: *The 9th Scandinavian Research Conference on Geographical Information Science*. Espoo: Helsinki University of Technology, 2003, pp. 251-259. ISBN 978-951-22-6565-7.

[23] MCCULLOUGH, M., P. JAYAKUMAR, J. DASCH and D. GORSICH. Next-Generation NATO Reference Mobility Model Development. *Journal of Terramechanics*, 2017, **73**, pp. 49-60. DOI 10.1016/j.jterra.2017.06.002.

[24] CHOI, S., J. PARK, E. LIM and W. YU. Global Path Planning on Uneven Elevation Maps. In: *2012 9th International Conference on Ubiquitous Robots and Ambient Intelligence (URAI)*. Daejeon: IEEE, 2012, pp. 49-54. DOI 10.1109/ URAI.2012.6462928.

[25] GANGANATH, N., C.T. CHENG and C.K. TSE. Finding Energy-Efficient Paths on Uneven Terrains. In: *2014 10th France-Japan/8th Europe-Asia Congress on Mecatronics*. Tokyo: IEEE, 2014, pp. 383-388. DOI 10.1109/ MECATRON-ICS.2014.7018555.

[26] RAJA, R., A. DUTTA and K.S. VENKATESH. New Potential Field Method for Rough Terrain Path Planning Using Genetic Algorithm for a 6-wheel Rover. *Robotics and Autonomous Systems*, 2015, **72**, pp. 295-306. DOI 10.1016 /j.robot.2015.06. 002.

[27] ZHANG, B., G. LI, Q. ZHENG, X. BAI, Y. DING and A. KHAN. Path Planning for Wheeled Mobile Robot in Partially Known Uneven Terrain. *Sensors*, 2022, **22**(14), 5217. DOI 10.3390 /s22145217.

[28] RADA, J., M. RYBANSKY and F. DOHNAL. The Impact of the Accuracy of Terrain Surface Data on the Navigation of Off-Road Vehicles. *ISPRS International Journal of Geo-Information*, 2021, **10**(3), 106. DOI 10.3390/ ijgi10030106.

[29] HU, H., J. GAO and P. HU. The Digital Generalization Principle of Digital Elevation Model. In: *Proceedings of SPIE*. Wuhan: SPIE, 2009, pp. 1-8. DOI 10.1117/12.838546.

[30] AI, T. and J. LI. A DEM Generalization by Minor Valley Branch Detection and Grid Filling. *ISPRS Journal of Photogrammetry and Remote Sensing*, 2010, **65**(2), pp. 198-207. DOI 10.1016/j.isprsjprs.2009.11.001.

[31] LI, J., Y. SHEN, A. GAO, K. CHEN, Y. ZHANG and T. AI. A Heuristic DEM Generalization by Combining Catchments. *Geocarto International*, 2021, **37**(25), pp. 9392-9407. DOI 10.1080/10106049.2021.2017019.

[32] DAWID, W. and K. POKONIECZNY. Analysis of the Possibilities of Using Different Resolution Digital Elevation Models in the Study of Microrelief on the Example of Terrain Passability. *Remote Sensing,* 2020, **12**(24), 4146. DOI 10.3390/rs12244146.

[33] JAVAID, M.A. Understanding Dijkstra's Algorithm. *SSRN Electronic Journal*, 2013. DOI 10.2139/ssrn.2340905.